



1 **On Coupled Unsaturated-Saturated Flow Process Induced by Vertical,**
2 **Horizontal and Slant Wells in Unconfined Aquifers**

3

4 Xiuyu Liang^{a*}, Hongbin Zhan^{b*}, You-Kuan Zhang^c, Jin Liu^a

5

6 ^aSchool of Earth Sciences and Engineering, Nanjing University,

7 Nanjing, Jiangsu 210093, P.R. China(xyliang@nju.edu.cn)

8 ^bDepartment of Geology & Geophysics, Texas A&M University, College Station, TX 77843-

9 3115, USA. (zhan@geos.tamu.edu)

10 ^cSchool of Environment Sciences and Engineering,

11 South University of Sciences and Technology of China,

12 Shenzhen, Guangdong 518055, P.R. China

13

14 *Co-corresponding authors

15

16

17

18

19 Submitted to *Hydrology and Earth System Sciences*

20 September, 2016

21



22 **Abstract**

23 Conventional models of pumping tests in unconfined aquifers often neglect the unsaturated flow
24 process. This study concerns coupled unsaturated-saturated flow process induced by vertical,
25 horizontal, and slant wells positioned in an unconfined aquifer. A mathematical model is
26 established with special consideration of the coupled unsaturated-saturated flow process and well
27 orientation. Groundwater flow in the saturated zone is described by a three-dimensional
28 governing equation, and a linearized three-dimensional Richards' equation in the unsaturated
29 zone. A solution in Laplace domain is derived by the Laplace-finite Fourier transform and the
30 method of separation of variables. It is found that the unsaturated zone has significant effects on
31 the drawdown of pumping test with any angle of inclination of the pumping well, and this impact
32 is more significant for the case of a horizontal well. The effects of unsaturated zone on the
33 drawdown are independent of the length of the horizontal well screen. For the early time of
34 pumping, the water volume drained from the unsaturated zone (W) increases with time, and
35 gradually approaches an asymptotic value with time progress. The vertical well leads to the
36 largest W value during the early time, and the effects of the well orientation become insignificant
37 at the later time. The screen length of the horizontal well does not affect W for the whole
38 pumping period. The proposed solutions are useful for parameter identification of pumping tests
39 with a general well orientation (vertical, horizontal, and slant) in unconfined aquifers affected
40 from above by the unsaturated flow process.

41

42 **Keywords:** Horizontal well; Slant well; Coupled unsaturated-saturated flow; Drainage from the
43 unsaturated zone.



44 **1. Introduction**

45 In addition to conventional vertical wells, horizontal and slant pumping wells are broadly
46 used in the petroleum industry, environmental and hydrological applications in recent decades.
47 Horizontal and slant pumping wells are commonly installed in shallow aquifers to yield a large
48 amount of groundwater (Bear, 1979) or to remove a large amount of contaminant (Sawyer and
49 Lieuallen-Dulam, 1998). Horizontal and slant wells have some advantages over vertical wells
50 (Yeh and Chang, 2013; Zhan and Zlotnik, 2002), e.g., horizontal and slant wells yield smaller
51 drawdowns than the vertical wells with the same pumping rate per screen length. Horizontal and
52 slant wells have long screen sections which can extract a great volume of water in shallow or low
53 permeability aquifers without generating significant drawdowns there.

54 Hantush and Papadopoulos (1962) firstly investigated the problem of fluid flow to a horizontal
55 well in hydrologic sciences. Since then, this problem was not of great concern in the
56 hydrological science community because of the limitation of directional drilling techniques and
57 high drilling costs. With significant advances of the directional drilling technology over the last
58 20 years, the interest of horizontal and/or slant wells was reignited. Until now flow to horizontal
59 and/or slant wells have been investigated in various aspects, including flow in confined aquifers
60 (Cleveland, 1994; Zhan, 1999; Zhan et al., 2001; Kompani-Zare et al., 2005), unconfined aquifers
61 (Huang et al., 2016; Rushton and Brassington, 2013; Zhan and Zlotnik, 2002; Huang et al.,
62 2011; Mohamed and Rushton, 2006; Kawecki and Al-Subaikhy, 2005), leaky confined aquifers
63 (Zhan and Park, 2003; Sun and Zhan, 2006; Hunt, 2005), and fractured aquifers (Nie et al.,
64 2012; Park and Zhan, 2003; Zhao et al., 2016). The readers can consult Yeh and Chang (2013) for
65 a recent review of well hydraulics on various well types, including horizontal and slant wells.



66 As demonstrated in previous studies, horizontal and slant wells had significant advantages
67 over vertical wells in unconfined aquifers, thus they were largely used in unconfined aquifers for
68 pumping or drainage purposes. However, none of above-mentioned studies considered the effect
69 of unsaturated process on groundwater flow to horizontal and slant wells in unconfined aquifers.
70 For the case of flow to vertical wells in saturated zones, the effects of above unsaturated
71 processes were investigated by several researchers (Kroszynski and Dagan, 1975; Mathias and
72 Butler, 2006; Tartakovsky and Neuman, 2007; Mishra and Neuman, 2010, 2011). For example,
73 Tartakovsky and Neuman (2007) considered axisymmetric saturated-unsaturated flow for a
74 pumping test in an unconfined aquifer and employed one parameter that characterized both the
75 water content and the hydraulic conductivity as functions of pressure head, assuming an infinite
76 thickness unsaturated zone. Mishra and Neuman (2010, 2011) extended the solution of
77 Tartakovsky and Neuman (2007) using four parameters to represent the unsaturated zone
78 properties and considering a finite thickness for the unsaturated zone (Mishra and Neuman,
79 2010), and considered the wellbore storage as well (Mishra and Neuman, 2011). The main results
80 from the studies concerning vertical wells indicated that the unsaturated zone had a major impact
81 on the S-shaped drawdown type curves.

82 A following question to ask is that are these conclusions drawn for vertical wells also
83 applicable for horizontal and slant wells when coupled unsaturated-saturated flow is of concern?
84 Specifically, how important is the wellbore orientation on groundwater flow to a horizontal or
85 slant well considering the coupled unsaturated-saturated flow process?
86 In order to answer these questions, we establish a mathematical model for groundwater flow to a
87 general well orientation (vertical, horizontal, and slant wells) considering the coupled
88 unsaturated-saturated flow process. We incorporate a three-dimensional linearized Richards'



89 equation into a governing equation of groundwater flow in an unconfined aquifer. We employ the
90 Laplace-finite Fourier transform and the method of separation of variables to solve the coupled
91 unsaturated-saturated flow governing equations. This paper is organized as follows, we first
92 present the mathematical model and solution in sections 2 and 3, respectively, then describe the
93 results and discussion in section 4, and summarize this study and draw conclusions in section 5
94 finally.

95 **2. Mathematical Model**

96 The schematic diagrams of flow to horizontal and slant wells in an unsaturated-saturated
97 system are represented in Fig. 1a. and 1b, respectively. Similar to the conceptual model used by
98 Zhan and Zlotnik (2002), the origin of the Cartesian coordinate is located at the bottom of the
99 saturated zone with the z axis along the upward vertical direction and the x and y axes along the
100 principal horizontal hydraulic conductivity directions. The horizontal and slant wells screen are
101 located in the saturated zone with a distance z_w from the center point of the screen $(0, 0, z_w)$ to
102 the bottom of the saturated zone. The slant well has three inclined angles γ_x , γ_y , and γ_z with the
103 x , y , and z axis, respectively, and such three angles satisfying $\cos^2(\gamma_x) + \cos^2(\gamma_y) + \cos^2(\gamma_z) =$
104 1. The horizontal well is a specific case of the slant well when $\gamma_z = \pi/2$. The saturated zone is
105 assumed as an infinite lateral extent unconfined aquifer with a slightly compressibility, and is
106 spatially uniform and anisotropic (Tartakovsky and Neuman, 2007). The saturated zone is below
107 an initially horizontal water table at $z = d$, and unsaturated zone is above $z = d$ with thickness
108 b .

109 In order to solve the problem of groundwater flow to a horizontal or slant well, we first solve
110 the governing equation of the groundwater flow to a point sink. The mathematical model for



111 groundwater flow to a point sink (x_0, y_0, z_0) in a homogeneously anisotropic saturated zone is

112 given by

$$113 \quad K_x \frac{\partial^2 s}{\partial x^2} + K_y \frac{\partial^2 s}{\partial y^2} + K_z \frac{\partial^2 s}{\partial z^2} + Q \delta(x - x_0) \delta(y - y_0) \delta(z - z_0) = S_S \frac{\partial s}{\partial t}, \quad 0 \leq z < d, \quad (1a)$$

$$114 \quad s(x, y, z, 0) = 0, \quad (1b)$$

$$115 \quad \frac{\partial s}{\partial z}(x, y, z, t)|_{z=0} = 0, \quad (1c)$$

$$116 \quad \lim_{x \rightarrow \pm\infty} s(x, y, z, t) = \lim_{y \rightarrow \pm\infty} s(x, y, z, t) = 0, \quad (1d)$$

117 where s is the drawdown (the change in hydraulic head from the initial level) in the saturated
118 zone [L]; K_x , K_y and K_z are the saturated principal hydraulic conductivities in the x , y and z
119 directions, respectively [LT^{-1}]; Q is pumping rate (positive for pumping and negative for
120 injecting) [L^3T^{-1}]; $\delta(\cdot)$ is the Dirac delta function [L^{-1}]; S_S is the specific storage [L^{-1}]; d is the
121 saturated zone thickness [L].

122 Flow in the unsaturated zone induced by pumping in the unconfined aquifer is governed by
123 Richards' equation. Due to the nonlinear nature of Richards' equation, it is difficult to
124 analytically solve this equation except for some specific cases. Kroszynski and Dagan (1975)
125 proposed a first-order linearized unsaturated flow equation by expanding the dependent variable
126 in Richards' equation as a power series when the pumping rate was less than Kd^2 , where K is the
127 saturated hydraulic conductivity of a homogeneous media. The readers can find the details of the
128 linearized equation derivation in previous studies (Kroszynski and Dagan, 1975; Tartakovsky and
129 Neuman, 2007). With such a linearized treatment, it becomes possible to analytically solve the
130 equation of flow in the unsaturated zone. The linearized three-dimensional unsaturated flow
131 equation is adopted in this study as follows,

$$132 \quad k_0(z)K_x \frac{\partial^2 u}{\partial x^2} + k_0(z)K_y \frac{\partial^2 u}{\partial y^2} + K_z \frac{\partial}{\partial z} \left(k_0(z) \frac{\partial u}{\partial z} \right) = C_0(z) \frac{\partial u}{\partial t}, \quad d \leq z < d + b, \quad (2a)$$

$$133 \quad u(x, y, z, 0) = 0, \quad (2b)$$



$$134 \quad \frac{\partial u}{\partial z}(x, y, t)|_{z=d+b} = 0, \quad (2c)$$

$$135 \quad \lim_{x \rightarrow \pm\infty} u(x, y, z, t) = \lim_{y \rightarrow \pm\infty} u(x, y, z, t) = 0, \quad (2d)$$

$$136 \quad k_0(z) = k(\theta_0), \quad C_0(z) = C(\theta_0), \quad (2e)$$

137 where u is the drawdown in the unsaturated zone [L]; the functions $k_0(z)$ and $C_0(z)$ are the
 138 zero-order approximation of the relative hydraulic conductivity [dimensionless] and the soil
 139 moisture capacity [L^{-1}] at the initial water content of θ_0 , respectively; k is the relative hydraulic
 140 conductivity and $0 \leq k \leq 1$; $C(\geq 0)$ is the specific moisture capacity [L^{-1}], and $C = d\theta/d\psi$, θ
 141 is the volumetric water content, and ψ is the pressure head [L]; b is the thickness of the
 142 unsaturated zone [L]. Similar to Tartakovsky and Neuman (2007), the unsaturated medium
 143 properties are described with the two-parameter Gardner (1958) exponential constitutive
 144 relationships,

$$145 \quad k_0(z) = e^{\kappa(d-z)}, \quad (3a)$$

$$146 \quad C_0(z) = S_y \kappa e^{\kappa(d-z)}, \quad (3b)$$

147 where $\kappa > 0$ is the constitutive exponent [L^{-1}], S_y is the specific yield [dimensionless]. It shows in
 148 Eq. (3b) that at the water table ($z=d$) a smaller κ leads to a smaller $C_0(z)$ and a larger retention
 149 capacity (Kroszynski and Dagan, 1975; Tartakovsky and Neuman, 2007), i.e., water in the
 150 unsaturated zone becomes more difficult to drain. In this study, we assume the upper boundary of
 151 the unsaturated zone as a no-flow boundary condition in Eq. (2c) by neglecting the effects of
 152 both infiltration and evaporation during the pumping. Because typical pumping tests usually last
 153 over much short periods of time relative to the time durations of infiltration and evaporation
 154 processes, this assumption can hold for most field conditions, particularly for lands with sparse
 155 vegetation where plant transpiration effect is limited as well.



156 The saturated and unsaturated flow are coupled at their interface by continuities of pressure
 157 and vertical flux across the water table which, following linearization, take the form

$$158 \quad s - u = 0, \quad z = b, \quad (4a)$$

$$159 \quad \frac{\partial s}{\partial z} - \frac{\partial u}{\partial z} = 0, \quad z = b. \quad (4b)$$

160 Above linearized equations of (4a) and (4b) assume that the variation of water table is minor
 161 in respect to the total saturated thickness. This assumption works better for horizontal wells and
 162 slant wells as for vertical wells, provided that the same pumping rate is used. This is because
 163 horizontal wells and slant wells will generate much less drawdowns over laterally broader regions;
 164 while vertical wells tend to generate laterally more concentrated and much greater drawdown near
 165 the pumping wells (Zhan and Zlotnik, 2002).

166 3. Solutions

167 3.1 Solution for a point sink

168 The solution to Eq. (1a) is obtained by the Laplace and finite cosine Fourier transform. The
 169 Laplace domain solution of Eq. (1a) subject to initial condition Eq. (1b) and boundary conditions
 170 Eqs. (1c) and (1d) is given as (Zhan and Zlotnik, 2002)

$$171 \quad \bar{s}_D(\mathbf{r}_D, z_D, p) = \sum_{n=0}^{\infty} \frac{8 \cos(\omega_n z_{0D}) \cos(\omega_n z_D)}{p \Psi(\omega_n)} K_0(\Omega_n |\mathbf{r}_D - \mathbf{r}_{0D}|), \quad (5)$$

172 where

$$173 \quad \Omega_n = \sqrt{\omega_n^2 + p}, \quad \Psi(\omega_n) = 2\alpha_z + \sin(2\omega_n \alpha_z) / \omega_n, \quad (6)$$

174 where the subscript D denotes the dimensionless terms, the definition of all dimensionless
 175 variables are presented in the supplementary material (S1); p is the Laplace transform parameter
 176 in respect to the dimensionless time, and the overbar denote a variable in the Laplace domain; ω_n
 177 is the n -th eigenvalue of the Fourier transform, and it will be determined later; K_0 is the modified



178 second-kind Bessel function of zero-order; $\mathbf{r}_D = (x_D, y_D)$ and $\mathbf{r}_{0D} = (x_{0D}, y_{0D})$ are
 179 dimensionless radial vectors of the observation and sink point, respectively.

180 The solution to Eq. (2a) is obtained by the Laplace transform and the method of separation of
 181 variables (supplementary material, S2) and is given as

$$182 \quad \bar{u}_D(r_D, z_D, p) = \sum_{n=0}^{\infty} \frac{8 \cos(\omega_n z_{0D})}{p \Psi(\omega_n)} K_0(\Omega_n |\mathbf{r}_D - \mathbf{r}_{0D}|) \mathcal{H}_n(z_D, p), \quad (7)$$

183 where

$$184 \quad \mathcal{H}_n = \begin{cases} \cos(\omega_n \alpha_z) \frac{(M+N) \exp[2N(\alpha_z+b_D)+(M-N)z_D] - (M-N) \exp[(M+N)z_D]}{(M+N) \exp[2N(\alpha_z+b_D)+(M-N)\alpha_z] - (M-N) \exp[(M+N)\alpha_z]}, & \text{if } \Delta > 0 \\ \cos(\omega_n \alpha_z) \exp(Mz_D - M\alpha_z) \frac{[N_1 \tan(N_1(\alpha_z+b_D)) - M] \sin(N_1 z_D) + [M \tan(N_1(\alpha_z+b_D)) + N_1] \cos(N_1 z_D)}{[N_1 \tan(N_1(\alpha_z+b_D)) - M] \sin(N_1 \alpha_z) + [M \tan(N_1(\alpha_z+b_D)) + N_1] \cos(N_1 \alpha_z)}, & \text{if } \Delta < 0 \\ \cos(\omega_n \alpha_z) \exp(Mz_D - M\alpha_z) \frac{1+M(\alpha_z+b_D)-Mz_D}{1+M(\alpha_z+b_D)-M\alpha_z}, & \text{if } \Delta = 0 \end{cases} \quad (8)$$

185 where $M = \kappa_D/2$; $N = \sqrt{\Delta}$ if $\Delta \geq 0$; $N_1 = \sqrt{-\Delta}$ if $\Delta < 0$; $\Delta = \kappa_D^2/4 + \beta p - \Omega_n^2$.

186 The eigenvalues of the finite cosine Fourier transform ω_n can be obtained by substituting
 187 Eqs. (5) and (7) into the continuities of normal (vertical) flux equation (Eq. (S6b)). The detail can
 188 be found in supplementary material (S3). On the basis of the method illustrated above, it is
 189 straightforward to obtain the Laplace domain solutions \bar{s}_D for the case of the unconfined aquifer
 190 with a free water table boundary and without the unsaturated zone influence (Zhan and Zlotnik,
 191 2002) (abbreviated as the ZZ solution hereinafter), and the case of the water flow to a horizontal
 192 well in an confined aquifer (Zhan et al., 2001) (abbreviated as the ZWP solution hereinafter). The
 193 solutions \bar{s}_D for these two special cases require different ω_n values. For the free water table
 194 condition the ω_n is the root of $\omega_n \tan(\omega_n) = p/\sigma$ (Zhan and Zlotnik, 2002). For the confined
 195 aquifer case the $\omega_n = n\pi/\alpha_z$, $n = 0, 1, 2, \dots$ (Zhan et al., 2001).

196 3.2 Solution for a slant pumping well

197 On the basis of the principle of superposition, the drawdown induced by a line sink in the
 198 saturated zone can be obtained by integrating the solution Eqs. (5) and (7) along the well axis,
 199 provided that the pumping strength distribution along the well screen is known. Precise



200 determination of the pumping strength distribution along a horizontal or slant well involves
 201 complex, coupled aquifer-pipe flow (Chen et al., 2003) in which the flow inside the wellbore
 202 (pipe flow) can experience different stages of flow schemes from laminar, transitional turbulent,
 203 to fully developed turbulent flow (Chen et al., 2003). However, often time one may adopt a first-
 204 order approximation of using a uniform flux distribution to treat the horizontal or slant wells,
 205 particularly when the well screen lengths are not extremely long (like kilometers). Such an
 206 approximation has been justified by Zhan and Zlotnik (2002). In this study, a uniform flux
 207 distribution will be utilized for horizontal or slant wells hereinafter to obtain the solutions.

208 The drawdown in saturated and unsaturated zones due to a slant pumping well can be written
 209 as:

$$210 \quad \bar{s}_{ID}(p) = \sum_{n=0}^{\infty} \frac{8 \cos(\omega_n z_D)}{L_D p \Psi(\omega_n)} \int_{-\frac{L_D}{2}}^{\frac{L_D}{2}} \cos \left[\omega_n \left(z_{wD} + l \frac{\alpha_z}{\alpha_x} \cos \gamma_z \right) \right] K_0[\Omega_n F(l)] dl, \quad (9)$$

211 and

$$212 \quad \bar{u}_{ID}(p) = \sum_{n=0}^{\infty} \frac{8 \mathcal{H}_n(z_D, p)}{L_D p \Psi(\omega_n)} \int_{-\frac{L_D}{2}}^{\frac{L_D}{2}} \cos \left[\omega_n \left(z_{wD} + l \frac{\alpha_z}{\alpha_x} \cos \gamma_z \right) \right] K_0[\Omega_n F(l)] dl, \quad (10)$$

213 respectively, where \bar{s}_{ID} and \bar{u}_{ID} are the Laplace transform of s_{ID} and u_{ID} , respectively, and they
 214 are defined in the same way as s_D and u_D in Eqs. (5) and (7), respectively; $L_D = \alpha_x L/d$ is the
 215 dimensionless length of the slant well screen (L); $z_{wD} = \alpha_z z_w/d$ is the dimensionless elevation of
 216 the center of the pumping well screen; l is a dummy variable; $F(l) =$
 217 $\sqrt{(x_D - l \sin \gamma_z \cos \gamma_x)^2 + (y_D - l \frac{\alpha_y}{\alpha_x} \sin \gamma_z \cos \gamma_y)^2}$. \bar{s}_{ID} and \bar{u}_{ID} will respectively reduce to
 218 drawdowns in the saturated and unsaturated zones due to a horizontal well when $\gamma_z = \pi/2$.

219 The drawdown in an observation (vertical) well located in the saturated zone that is screened
 220 from z_l to z_u ($z_u > z_l$) can be calculated using the average of the point drawdown Eq. (9) along
 221 the observation well screen (Zhan and Zlotnik, 2002):



$$\bar{s}_{oD}(p) = \sum_{n=0}^{\infty} \frac{8[\sin(\omega_n z_{uD}) - \sin(\omega_n z_{lD})]}{L_D(z_{uD} - z_{lD})\omega_n p \Psi(\omega_n)} \int_{-\frac{L_D}{2}}^{\frac{L_D}{2}} \cos\left[\omega_n \left(z_{wD} + l \frac{\alpha_z}{\alpha_x} \cos \gamma_z\right)\right] K_0[\Omega_n F(l)] dl, \quad (11)$$

where \bar{s}_{oD} is the Laplace transform of s_{oD} , and s_{oD} is defined in the same way as s_D in Eq. (5);

$$z_{uD} = \alpha_z z_u / d, \quad z_{lD} = \alpha_z z_l / d.$$

3.3 Total volume drained from the unsaturated zone for a slant well

The dimensionless total volume drained from the unsaturated zone to the saturated zone (water flux across the water table) can be obtained by

$$\bar{W}_D(p) = - \int_{-\infty}^{+\infty} \int_{-\infty}^{+\infty} \frac{\partial \bar{s}_{lD}}{\partial z_D} \Big|_{\alpha_z} dx_D dy_D = \sum_{n=0}^{\infty} \frac{16\pi \sin(\omega_n \alpha_z) \cos(\omega_n z_{wD}) \sin(\omega_n \phi)}{p \Psi(\omega_n) \Omega_n^2 \phi}, \quad (12)$$

where \bar{W}_D is the Laplace transform of W_D , and $W_D = W \frac{4\pi \alpha_z^3}{Q}$, W is the total volume drained from the unsaturated zone; $\phi = L_D \alpha_z \cos \gamma_z / (2\alpha_x)$.

It is difficult to obtain closed-form solutions by analytically inverting the Laplace transforms of Eqs. (5), (7), (9), (10) and (12) and thus numerical inverse Laplace method is employed in this study. There are several numerical inverse Laplace methods, such as Stehfest method (Stehfest, 1970), Zakian method (Zakian, 1969), Fourier series method (Dubner and Abate, 1968), Talbot algorithm (Talbot, 1979), Crump technique (Crump, 1976), and de Hoog algorithm (de Hoog et al., 1982), with each method best fitted for a particular type of problem (Hassanzadeh and Pooladi-Darvish, 2007). The Stehfest algorithm is sufficiently accurate for the flow problem studied here. Chen (1985), Zhan et al. (2009a; 2009b), and Wang and Zhan (2013) have successfully employed the Stehfest algorithm to obtain the real-time domain solution for the similar problems to this study. For references to different inverse Laplace methods, one can consult the review of Kuhlman (2013) and Wang and Zhan (2015). In this study we use the Stehfest method to invert the Laplace solutions into the real-time solutions. Extensive numerical



243 exercises have been performed to against the benchmark solutions for several special cases of the
244 investigated problem to ensure the degree of accuracy of the Stehfest method.

245 **4. Results and Discussion**

246 **4.1 Effect of unsaturated parameters**

247 The main difference between the ZZ solution and present solution is the upper boundary
248 condition of the saturated zone. The ZZ solution considered linearized kinematic equation as the
249 water table boundary that employed one parameter, i.e., specific yield (S_y) to account for the
250 gravity drainage after water table declining. The present solution represents coupled water flow
251 through both the unsaturated and saturated zones. The water table boundary is replaced by
252 coupled interface conditions between the unsaturated and the saturated zones. Thus the behavior
253 of the drawdown in the saturated zone induced by the pumping wells will be affected by the
254 unsaturated zone. To investigate the manner in the dimensionless constitutive exponent κ_D and
255 the dimensionless unsaturated thickness b_D impact the drawdown in the saturated zone induced
256 by a horizontal pumping well, we plot the log-log graph of s_{ID} versus the dimensionless time
257 t_D/r_D^2 (the type curves) for different κ_D and b_D in Figures 2a and 2b, respectively. We also
258 compare our solution to the ZZ solution (unconfined aquifer) and the ZWP solution (confined
259 aquifer). For the convenience we assume the horizontal well screen along the x -direction, i.e.,
260 $\gamma_x = 0$ and $\gamma_y = \gamma_z = \pi/2$. The others parameter values in Eq. (9) are $\sigma=1\times 10^{-3}$, $L_D=1$, $\gamma=0$,
261 $\alpha_z=1$, $x_D=0.5$, $y_D=0.05$, $z_D=0.8$, and $z_{wD}=0.5$.

262 Figure 2a presents the drawdown curves in the saturated zone for different values of κ_D
263 (1×10^{-5} , 1×10^{-3} , 1×10^{-1} , 1×10^1 and 1×10^3) with a fixed dimensionless thickness of the
264 unsaturated zone b_D of 0.5. It shows that the unsaturated zone has significant impact on



265 drawdown curves. Our curve is almost the same as the curve of the ZZ solution when $\kappa_D = 1 \times 10^3$
266 (gray solid curve), and gradually deviates from the ZZ solution but approaches the ZWP solution
267 as κ_D decreases to 1×10^{-5} (black solid curve). The dimensionless constitutive exponent $\kappa_D =$
268 $\kappa d / \alpha_z = \kappa d K_D^{1/3}$, where K_D is the anisotropic rate between the vertical hydraulic conductivity
269 (K_z) and the horizontal hydraulic conductivity (K_r).

270 For smaller κ_D the unsaturated zone has larger retention capacity, the saturated zone has
271 smaller initial saturated thickness, and/or both the unsaturated and saturated zones have
272 relatively smaller vertical hydraulic conductivity, leading to less impacts on the drawdown in the
273 saturated zone. Such effect increases as κ_D increases, and becomes significant at κ_D greater than
274 10. For a fixed initial saturated thickness, when κ_D is smaller, i.e., the unsaturated zone has larger
275 retention capacity and/or both the unsaturated and saturated zones have relatively small vertical
276 hydraulic conductivity, water drainage from the unsaturated zone is impeded, forcing more water
277 to be released from compressible storage of the saturated zone, leading to large drawdown in the
278 saturated zone. The opposite is true when κ_D is larger. It is consistent with the findings in the
279 vertical pumping well case (Tartakovsky and Neuman, 2007).

280 It also shows in Figure 2a that the drawdown have typical “S” pattern curves while $\kappa_D \geq 0.1$.
281 At early time all curves are approximately identical due to response of the confined storage and
282 little effects of the upper boundary of the saturated zone; at intermediate time the drawdowns of
283 the ZZ solution and our solutions increase slower than that of the ZWP solution due to response
284 of additional storage (water table boundaries and unsaturated zone) of the upper boundary of the
285 saturated zone; at late time the drawdown increasing rates of the ZZ solution and our solutions
286 are nearly the same as that of the ZWP solution due to the combined effects of both storage
287 mechanisms.



288 The unsaturated zone controls the effects of additional storage and upper boundary of the
289 saturated zone on drawdown curves. There are physical differences between the ZZ solution and
290 our solution. The ZZ solution uses the storage factor S_y (specific yield) at upper boundary of the
291 saturated zone. Such a storage factor at the upper boundary is greater than the actual storage
292 capacity of the unsaturated zone when the unsaturated parameter $\kappa_D \leq 10$, leading to a slower
293 water level decline for the ZZ solution, and such effect will become insignificant for a long
294 pumping time. Similar to κ_D , the dimensionless unsaturated thickness b_D also has a significant
295 impact on the drawdown, as shown in Figure 2b for different values of b_D (0.001, 0.01, 1, 10 and
296 100) with a fixed $\kappa_D=0.1$ and the same parameters used as Figure 2a. Figure 2b shows that our
297 solution approaches the ZWP solution when $L_D=0.001$. For the large b_D (=100), however, our
298 solution is significantly different from the ZZ solution at intermediate time because the impact of
299 unsaturated flow becomes significant at a fixed κ_D of 0.1.

300 4.2 Effect of well orientation and well screen length

301 In this section, we first investigate the effect of the inclined angle of the slant well on the type
302 curves. Figure 3 shows the comparison between the ZZ solution and our solution with $\kappa_D = 10$
303 for three different angles of a slant well ($\gamma_z = 0, \pi/4$, and $\pi/2$) at two observation points ($z_D =$
304 0.9 for Figure 3a and $z_D = 0.1$ for Figure 3b) where the other parameters are the same as in
305 Figure 2. Obviously the smaller angle creates the larger drawdown at both observation points.
306 For the horizontal well ($\gamma_z = \pi/2$) the discrepancy between the ZZ solution and our solution is
307 larger than that for the vertical well ($\gamma_z = 0$) at upper observation point (Figure 3a). Such a
308 discrepancy is also found at the lower observation point (Figure 3b). It reveals that the
309 unsaturated zone has significant effects on the drawdown for any angle of inclination of a slant
310 well, and this impact is more significant for the case of the horizontal well.



311 Here we investigate the effect of the horizontal well screen length on the drawdown. Figure
312 4 illustrates the comparison between the ZZ solution and our solution for three different length of
313 well screen ($L_D = 0.1, 1, \text{ and } 10$) at two observation points where the other parameters are the
314 same as in Figure 3. It indicates that the longer well screen leads to the smaller drawdown at both
315 upper and lower observation points. The discrepancy between the ZZ solutions and our solutions
316 are identical for different well screen lengths. It reveals that the effects of the unsaturated zone
317 on the drawdown are insensitive to the length of the horizontal well screen.

318 In order to further illustrate the drawdown pattern in the saturated zone. The profile of
319 drawdown in vertical cross-section for three different angles of a slant well ($\gamma_z = 0, \pi/4, \text{ and } \pi/2$)
320 at different dimensionless times ($t_D = 1 \times 10^3, 1 \times 10^4, \text{ and } 1 \times 10^5$) are presented in Figure 5.
321 The other parameter values in Eqs. (9) and (10) are $\sigma = 1 \times 10^{-5}, \kappa_D = 1 \times 10^3, L_D = 0.5, \alpha_z = 1, b_D = 1,$
322 $y_D = 0.05, z_{wD} = 0.75, \gamma_x = 0, \text{ and } \gamma_y = \pi/2$. As time increases, the effect of pumping gradually
323 propagates into the unsaturated zone ($z_D > 1$). The vertical well leads to larger drawdown in the
324 unsaturated zone than the slant and horizontal wells. The reason is that the vertical well screen is
325 more close to the unsaturated zone.

326 The water flux across water table (Eq. (12)) is the volume drained from the unsaturated zone
327 to the saturated zone. It is somewhat related to the concept of specific yield when the coupled
328 unsaturated-saturated zone flow process is simplified into a saturated zone flow process with
329 water table served as a free upper boundary. Thus, Eq. (12) reflects the impacts of the
330 unsaturated zone on the water flow in the saturated zone. Figure 6 shows the changes of the
331 dimensionless water flux across water table, W_D , with t_D of the ZZ solution and our solution at
332 three angles of a slant well screen ($\gamma_z = 0, \pi/4, \text{ and } \pi/2$) (Figure 6a), and at three screen lengths



333 of a horizontal well ($L_D = 0.1, 1.0, \text{ and } 10$) (Figure 6b), where the other parameters are the same
334 as in Figure 3.

335 At the early time of pumping, W_D increases with time, and at the later time W_D approaches
336 an asymptotic value that is dependent on the unsaturated parameter κ_D . W_D decreases with κ_D
337 decreasing. The small κ_D reflects the large retention capacity of the unsaturated zone, and thus it
338 impedes more water draining from the unsaturated zone during pumping. It results in more water
339 releasing from the saturated zone storage and larger drawdown in the saturated zone (Figure 2a).
340 The ZZ solution overestimates W_D due to the fact that it neglects the effects of above unsaturated
341 flow (Figure 6a). The $W_D \sim t_D$ curves deviate from each other considerably for different angles of
342 a slant well, particularly at the early time. One can see from Figure 6a that W_D of the vertical
343 well ($\gamma_z = 0$) is the largest at early time, and $W_D \sim t_D$ curves of three angles eventually approach
344 the same asymptotic value at late time. It means that the vertical well leads to the greatest water
345 drainage from the unsaturated zone at early time, and the effects of the well orientation are
346 insignificant with time increasing. Very different from the angle of a slant well, the screen length
347 of a horizontal well appears to have almost no impact on W_D for the whole pumping period
348 (Figure 6b). Similar with Figure 6a, the magnitude of W_D in Figure 6b is only dependent on the
349 unsaturated parameter κ_D .

350 **5. Summary and Conclusions**

351 The coupled unsaturated-saturated flow process induced by vertical, horizontal, and slant
352 pumping wells is investigated in this study. A mathematical model for such a coupled
353 unsaturated-saturated flow process is presented. The flow in the saturated zone is described by a
354 three-dimensional governing equation, and the flow in the unsaturated zone is described by a



355 three-dimensional Richards' equation. The unsaturated medium properties are represented by the
356 Gardner (1958) exponential relationships. The Laplace domain solutions are derived using
357 Laplace transform and the method of separation of variables, and the semi-analytical solutions
358 are obtained using the Stehfest method (Stehfest, 1970). The solution is compared with the
359 solutions proposed by Zhan et al. (2001) (confined aquifer, the ZWP solution) and Zhan and
360 Zlotnik (2002) (unconfined aquifer, the ZZ solution). The conclusions of this study can be
361 summarized as follows:

- 362 1) The unsaturated flow has significant impact on drawdown in unconfined aquifers induced by
363 the horizontal pumping well. The drawdown curves obtained in this study deviate from the ZZ
364 solution when considering the unsaturated flow effect. For the small dimensionless constitutive
365 exponent $\kappa_D (= 1 \times 10^{-5})$ (the large retention capacity of unsaturated zone, the small initial
366 saturated thickness, and/or the relatively small vertical hydraulic conductivity), the drawdown
367 curves approach the solution of the confined aquifer (the ZWP solution). For the large κ_D
368 $(= 1 \times 10^3)$, the drawdown curves approach the solution of the unconfined aquifer with the
369 linearized free water table boundary (the ZZ solution).
- 370 2) For the small dimensionless unsaturated thickness $b_D (= 0.001)$, the drawdown curves
371 approach the ZWP solution. For the large unsaturated thickness $b_D (= 100)$, the drawdown
372 curves do not approach the ZZ solution because the impact of the unsaturated flow becomes
373 significant at a fixed κ_D of 0.1.
- 374 3) The unsaturated zone has significant effects on the drawdown of the pumping test with any
375 angle of inclination of a slant well, and this impact is more significant for the case of the
376 horizontal well. The effects of the unsaturated zone on the drawdown are insensitive to the
377 length of the horizontal well screen.



378 4) For the early time of pumping, the water volume drained from the unsaturated zone (W) to the
379 saturated zone increases with time, and with time progressing, W approaches an asymptotic
380 value that is dependent on the unsaturated parameter κ_D . The vertical well leads to the largest
381 W value during the early time of pumping, and the effects of the well orientation become
382 insignificant at the later time. The screen length of the horizontal well does not affect W for the
383 whole pumping period.

384 **Acknowledgement**

385 This study was partially supported with the research grants from the National Nature Science
386 Foundation of China (NSFC-41330314; NSFC-41272260; NSFC-41302180), the National Key
387 project “Water Pollution Control” of China (2015ZX07204-007), and the Natural Science
388 Foundation of Jiangsu Province (BK20130571).

389



390 References

- 391 Bear, J.: Hydraulics of groundwater, McGraw-Hill series in water resources and environmental
392 engineering, McGraw-Hill International Book Co., London ; New York, xiii, 567 p. pp., 1979.
- 393 Chen, C. S.: Analytical and Approximate Solutions to Radial Dispersion from an Injection Well to a
394 Geological Unit with Simultaneous Diffusion into Adjacent Strata, *Water Resour Res*, 21, 1069-
395 1076, Doi 10.1029/Wr021i008p01069, 1985.
- 396 Chen, C. X., Wan, J. W., and Zhan, H. B.: Theoretical and experimental studies of coupled seepage-pipe
397 flow to a horizontal well, *J Hydrol*, 281, 159-171, 10.1016/s0022-1694(03)00207-5, 2003.
- 398 Cleveland, T. G.: Recovery Performance for Vertical and Horizontal Wells Using Semianalytical
399 Simulation, *Ground Water*, 32, 103-107, 10.1111/j.1745-6584.1994.tb00617.x, 1994.
- 400 Crump, K. S.: Numerical Inversion of Laplace Transforms Using a Fourier-Series Approximation, *J Acm*,
401 23, 89-96, Doi 10.1145/321921.321931, 1976.
- 402 de Hoog, F. R., Knight, J. H., and Stokes, A. N.: An Improved Method for Numerical Inversion of
403 Laplace Transforms, *Siam J Sci Stat Comp*, 3, 357-366, Doi 10.1137/0903022, 1982.
- 404 Dubner, H., and Abate, J.: Numerical Inversion of Laplace Transforms by Relating Them to Finite Fourier
405 Cosine Transform, *J Acm*, 15, 115-&, Doi 10.1145/321439.321446, 1968.
- 406 Gardner, W. R.: Some steady state solutions of unsaturated moisture flow equations with application to
407 evaporation from a water table, *Soil Sci.*, 85, 228-232, doi:10.1097/00010694-195804000-00006,
408 1958.
- 409 Hassanzadeh, H., and Pooladi-Darvish, M.: Comparison of different numerical Laplace inversion methods
410 for engineering applications, *Appl Math Comput*, 189, 1966-1981, DOI
411 10.1016/j.amc.2006.12.072, 2007.
- 412 Huang, C. S., Chen, Y. L., and Yeh, H. D.: A general analytical solution for flow to a single horizontal
413 well by Fourier and Laplace transforms, *Adv Water Resour*, 34, 640-648,
414 10.1016/j.advwatres.2011.02.015, 2011.
- 415 Huang, C. S., Chen, J. J., and Yeh, H. D.: Approximate analysis of three-dimensional groundwater flow
416 toward a radial collector well in a finite-extent unconfined aquifer, *Hydrol Earth Syst Sc*, 20, 55-71,
417 10.5194/hess-20-55-2016, 2016.
- 418 Hunt, B.: Flow to vertical and nonvertical wells in leaky aquifers, *J Hydrol Eng*, 10, 477-484,
419 10.1061/(asce)1084-0699(2005)10:6(477), 2005.
- 420 Kawecki, M. W., and Al-Subaikh, H. N.: Unconfined linear flow to a horizontal well, *Ground Water*, 43,
421 606-610, 2005.
- 422 Kompani-Zare, M., Zhan, H. B., and Samani, N.: Analytical study of capture zone of a horizontal well in
423 a confined aquifer, *J Hydrol*, 307, 48-59, 10.1016/j.hydrol.2004.09.021, 2005.



- 424 Kroszynski, U. I., and Dagan, G.: WELL PUMPING IN UNCONFINED AQUIFERS - INFLUENCE OF
425 UNSATURATED ZONE, *Water Resour Res*, 11, 479-490, 10.1029/WR011i003p00479, 1975.
- 426 Kuhlman, K. L.: Review of inverse Laplace transform algorithms for Laplace-space numerical
427 approaches, *Numer Algorithms*, 63, 339-355, 10.1007/s11075-012-9625-3, 2013.
- 428 Mathias, S. A., and Butler, A. P.: Linearized Richards' equation approach to pumping test analysis in
429 compressible aquifers, *Water Resour Res*, 42, 10.1029/2005wr004680, 2006.
- 430 Mishra, P. K., and Neuman, S. P.: Improved forward and inverse analyses of saturated-unsaturated flow
431 toward a well in a compressible unconfined aquifer, *Water Resour Res*, 46,
432 10.1029/2009WR008899, 2010.
- 433 Mishra, P. K., and Neuman, S. P.: Saturated-unsaturated flow to a well with storage in a compressible
434 unconfined aquifer, *Water Resour Res*, 47, 10.1029/2010WR010177, 2011.
- 435 Mohamed, A., and Rushton, K.: Horizontal wells in shallow aquifers: Field experiment and numerical
436 model, *J Hydrol*, 329, 98-109, 10.1016/j.jhydrol.2006.02.006, 2006.
- 437 Nie, R. S., Meng, Y. F., Jia, Y. L., Zhang, F. X., Yang, X. T., and Niu, X. N.: Dual Porosity and Dual
438 Permeability Modeling of Horizontal Well in Naturally Fractured Reservoir, *Transport Porous Med*,
439 92, 213-235, 10.1007/s11242-011-9898-3, 2012.
- 440 Park, E., and Zhan, H. B.: Hydraulics of horizontal wells in fractured shallow aquifer systems, *J Hydrol*,
441 281, 147-158, 10.1016/s0022-1694(03)00206-3, 2003.
- 442 Rushton, K. R., and Brassington, F. C.: Hydraulic behaviour and regional impact of a horizontal well in a
443 shallow aquifer: example from the Sefton Coast, northwest England (UK), *Hydrogeol J*, 21, 1117-
444 1128, 10.1007/s10040-013-0985-0, 2013.
- 445 Sawyer, C. S., and Lieuallen-Dulam, K. K.: Productivity comparison of horizontal and vertical ground
446 water remediation well scenarios, *Ground Water*, 36, 98-103, 10.1111/j.1745-6584.1998.tb01069.x,
447 1998.
- 448 Stehfest, H.: Numerical Inversion of Laplace Transforms, *Commun Acm*, 13, 47-&, Doi
449 10.1145/361953.361969, 1970.
- 450 Sun, D. M., and Zhan, H. B.: Flow to a horizontal well in an aquitard-aquifer system, *J Hydrol*, 321, 364-
451 376, 10.1016/j.jhydrol.2005.08.008, 2006.
- 452 Talbot, A.: Accurate Numerical Inversion of Laplace Transforms, *J I Math Appl*, 23, 97-120, 1979.
- 453 Tartakovsky, G. D., and Neuman, S. P.: Three-dimensional saturated-unsaturated flow with axial
454 symmetry to a partially penetrating well in a compressible unconfined aquifer, *Water Resour Res*,
455 43, 10.1029/2006WR005153, 2007.
- 456 Wang, Q. R., and Zhan, H. B.: Radial reactive solute transport in an aquifer-aquitard system, *Adv Water*
457 *Resour*, 61, 51-61, DOI 10.1016/j.advwatres.2013.08.013, 2013.



- 458 Wang, Q. R., and Zhan, H. B.: On different numerical inverse Laplace methods for solute transport
459 problems, *Adv Water Resour*, 75, 80-92, 10.1016/j.advwatres.2014.11.001, 2015.
- 460 Yeh, H. D., and Chang, Y. C.: Recent advances in modeling of well hydraulics, *Adv Water Resour*, 51, 27-
461 51, 10.1016/j.advwatres.2012.03.006, 2013.
- 462 Zakian, V.: Numerical Inversion of Laplace Transform, *Electron Lett*, 5, 120-&, Doi
463 10.1049/EI:19690090, 1969.
- 464 Zhan, H. B.: Analytical study of capture time to a horizontal well, *J Hydrol*, 217, 46-54, 10.1016/s0022-
465 1694(99)00013-x, 1999.
- 466 Zhan, H. B., Wang, L. V., and Park, E.: On the horizontal-well pumping tests in anisotropic confined
467 aquifers, *J Hydrol*, 252, 37-50, 10.1016/s0022-1694(01)00453-x, 2001.
- 468 Zhan, H. B., and Zlotnik, V. A.: Groundwater flow to a horizontal or slanted well in an unconfined
469 aquifer, *Water Resour Res*, 38, Artn 1108
470 Doi 10.1029/2001wr000401, 2002.
- 471 Zhan, H. B., and Park, E.: Horizontal well hydraulics in leaky aquifers, *J Hydrol*, 281, 129-146, Doi
472 10.1016/S0022-1694(03)00205-1, 2003.
- 473 Zhan, H. B., Wen, Z., and Gao, G. Y.: An analytical solution of two-dimensional reactive solute transport
474 in an aquifer-aquitard system, *Water Resour Res*, 45, Artn W10501
475 Doi 10.1029/2008wr007479, 2009a.
- 476 Zhan, H. B., Wen, Z., Huang, G. H., and Sun, D. M.: Analytical solution of two-dimensional solute
477 transport in an aquifer-aquitard system, *J Contam Hydrol*, 107, 162-174, DOI
478 10.1016/j.jconhyd.2009.04.010, 2009b.
- 479 Zhao, Y. Q., Zhang, Y. K., and Liang, X. Y.: Analytical solutions of three-dimensional groundwater flow
480 to a well in a leaky sloping fault-zone aquifer, *J Hydrol*, 539, 204-213,
481 10.1016/j.jhydrol.2016.05.029, 2016.
- 482



483

Figure captions

484 **Figure 1** The schematic diagram of groundwater flow to a horizontal well (a) and a slant well (b) in a
485 unsaturated-saturated system.

486 **Figure 2** a) log-log plot of s_{ID} against t_D/r_D^2 for different values of the dimensionless unsaturated
487 parameter κ_D , the ZWP solution (confined aquifer) and the ZZ solution (unconfined aquifer), and b) log-
488 log plot of s_{ID} against t_D/r_D^2 for different values of the dimensionless unsaturated thickness b_D , the ZWP
489 solution (confined aquifer) and the ZZ solution (unconfined aquifer).

490 **Figure 3** log-log plot of s_{ID} against t_D/r_D^2 for different angles of well screen and comparison with the ZZ
491 solution for a) dimensionless piezometer location (0, 0.05, 0.9), and b) dimensionless piezometer location
492 (0, 0.05, 0.1).

493 **Figure 4** log-log plot of s_{ID} against t_D/r_D^2 for different dimensionless lengths of horizontal well screen
494 and comparison with the ZZ solution for a) dimensionless piezometer location (0, 0.05, 0.9), and b)
495 dimensionless piezometer location (0, 0.05, 0.1).

496 **Figure 5** Vertical profiles of s_{ID} in saturated and u_{ID} in unsaturated zones for different angles of well
497 screen corresponding to various dimensionless times.

498 **Figure 6** log-log plot of W_D against t_D for different values of the dimensionless unsaturated parameter
499 κ_D and the ZZ solution with a) three angles of the slant well screen ($\gamma_z = 0, \pi/4, \text{ and } \pi/2$), and b) three
500 dimensionless lengths of the horizontal well screen ($L_D = 0.1, 1.0, \text{ and } 10$).

501

502



503
504
505

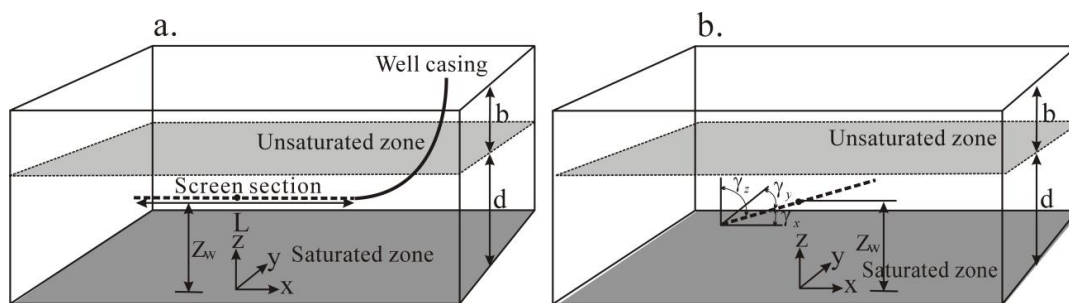
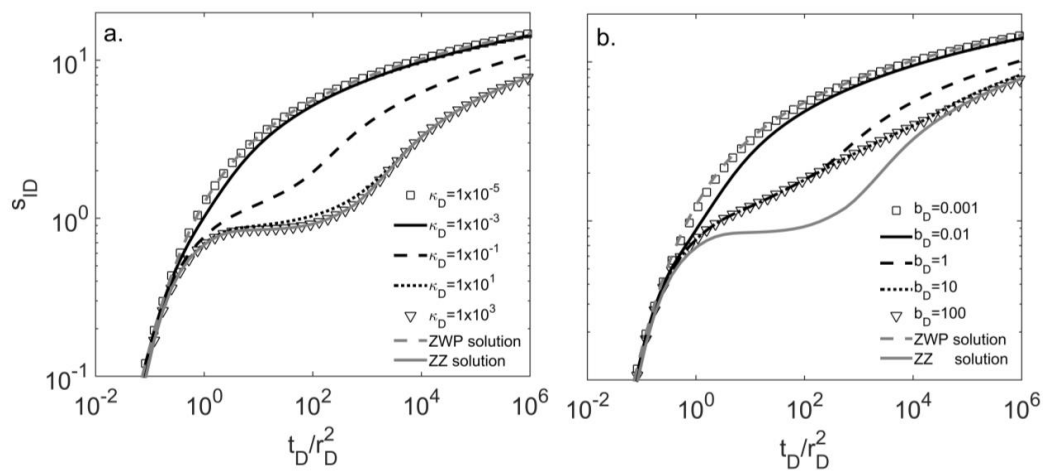


Figure 1



506



507

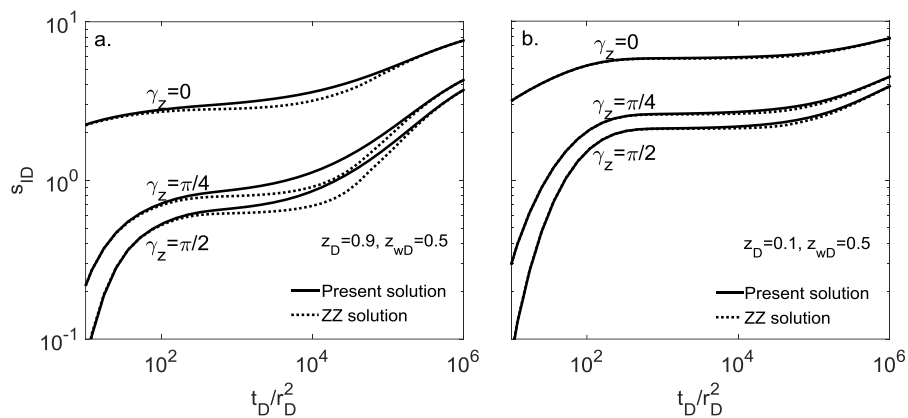
508

509

Figure 2



510



511

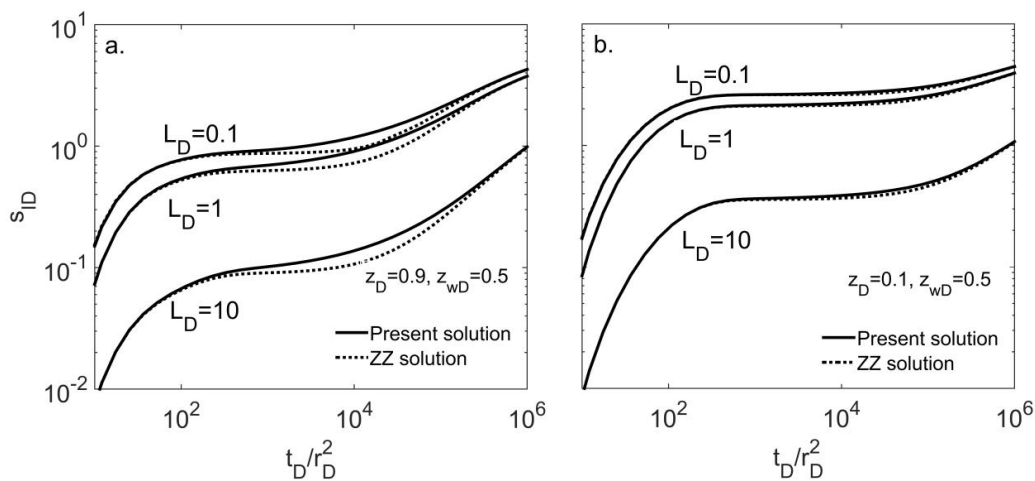
512

Figure 3

513



514



515

516

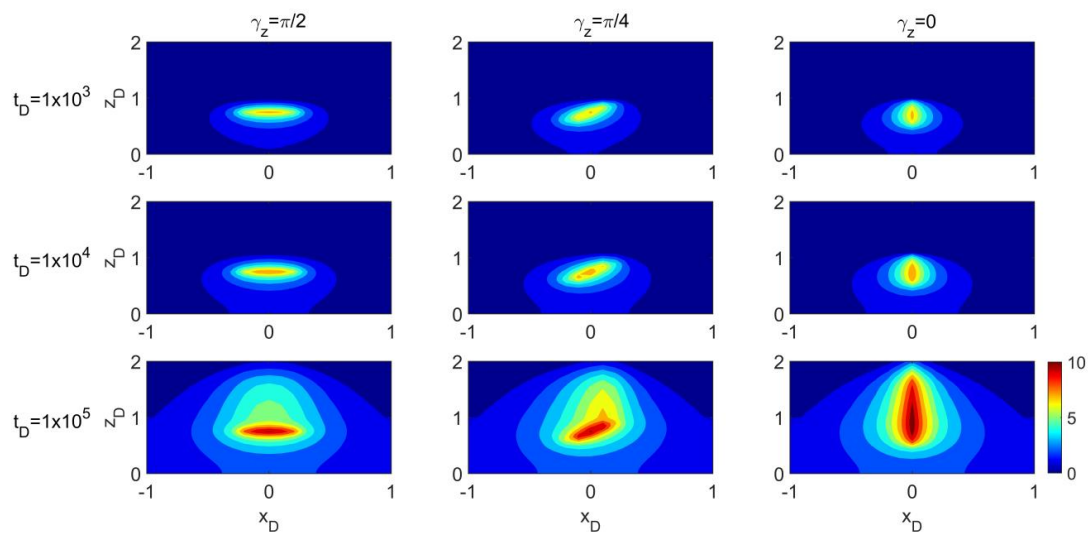
Figure 4

517

518



519

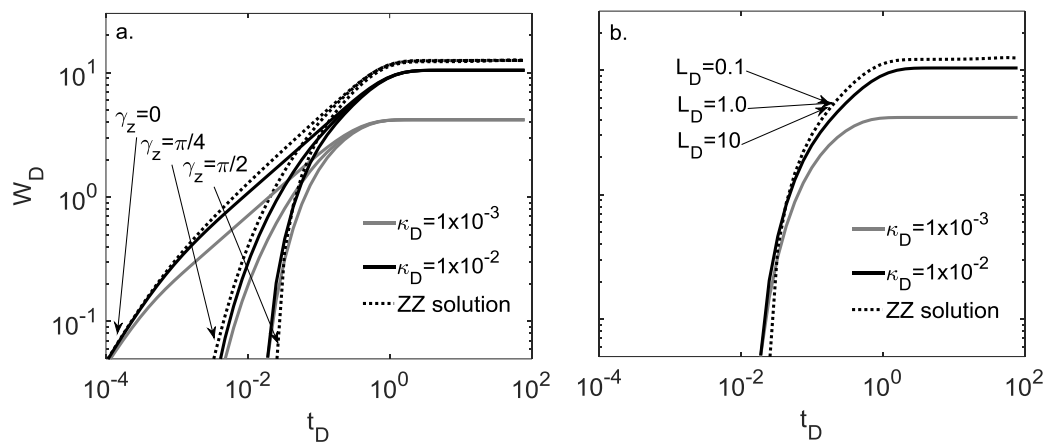


520

521

522

Figure 5



523

524

Figure 6

525